Study on improving regularity of neural phase locking in single neuron of AVCN via computational model

Kazuhito Ito and Masato Akagi

Japan Advanced Institute of Science and Technology

1 Introduction

One way of expressing temporal information in the auditory system is through the regularity of the interspike interval (ISI). This results from the firing of auditory nerve fibers (ANFs) being phase locked to the stimulation waveform (Johnson 1980). Consequently, ISIs represent periods corresponding to the reciprocals of their own characteristic frequencies (CFs). The temporal information of ISIs is thought to be used in various auditory perceptions such as sound localization based on the interaural time difference (ITD) and pitch perception. There may be a mechanism for transmitting accurate temporal information in the auditory system and this has been indicated by several psycho-physic studies where humans can detect small changes in the ITD within microseconds (Mills 1958). However, ANFs do not always fire in synchronization with a certain phase of the stimuli, and impulses on the fibers fluctuate slightly (similar to jitter) and occasionally pause. The degree of jitter in ANFs ranges from hundreds of microseconds to a few milliseconds (Johnson 1980). Consequently, there must be a mechanism responsible that improves temporal information on the auditory pathway. Recent physiological studies have found that bushy cells in the anteroventral cochlear nucleus (AVCN) have improved phase locking to low frequency tones (< 1 kHz) when compared to ANFs (Joris, Carney, Smith, and Yin 1994). In this paper, we demonstrate the mechanism through which a single cell improves the regularity of the ISI from the viewpoint of entrainment as well as synchronization using a computational model. We then discuss the relationship between the number of input terminals and the number of input events to maintain the ISI more regularly against the primary-like behavior of inputs from ANFs.

2 Synchronization and entrainment

The degree of phase locking in ANFs and neurons can be estimated with two scales, i.e., synchronization and entrainment. Synchronization is associated with how accurately spikes occur at a certain phase angle, and entrainment is associated with

how regularly spikes tune to each stimulus cycle. The synchronization index is calculated with the period histograms of spikes to tones at CF on individual cycles of the stimulus and defined through the following equations by Johnson (1980).

$$\hat{S}_f = (\hat{S}_{s,f}^2 + \hat{S}_{c,f}^2)^{1/2}, \quad \hat{S}_{s,f} = \frac{1}{N}\sum_{m=0}^{M-1} h_m \sin\frac{2\pi m}{M}, \quad \hat{S}_{c,f} = \frac{1}{N}\sum_{m=0}^{M-1} h_m \cos\frac{2\pi m}{M}, \quad (1)$$

where $\hat{S}_f$ indicates the estimated index, $\hat{S}_{s,f}$ and $\hat{S}_{c,f}$ denote the sine and cosine components of the period histogram, h_m ($m = 0, 1, ..., M\text{-}1$) denotes the content of the mth bin of a period histogram with M bins, and N denotes the number of spikes contained in the period histograms. Perfect alignment of all spikes in one bin yields an index value of 1, whereas a uniform distribution of spikes throughout the stimulus cycle yields a value of 0. The entrainment index is derived from the interspike interval histograms of spikes to measure the ability of fibers and neurons to respond with one spike for every stimulus cycle and defined by Joris et al. (1994).

$$E = h_F / N_s, \quad (2)$$

where E is the entrainment index, N_s denotes the total number of intervals of spikes during stimulation and h_F denotes the number of ISIs falling within a window equaling one stimulus period (1/CF). Perfect entrainment is achieved when a single spike occurs with each stimulus cycle and yields an index value of 1. If spikes are skipped some stimulus cycles, index values decrease. It is thus important to enhance temporal information so that it satisfies both synchronization and entrainment.

3 Physiological and anatomical properties of bushy cells

Mills (1958) found that some listeners could detect interaural time difference within microseconds in his psycho-physic experiments. This suggests there is a capability to transmit temporal information accurately in the auditory system. Johnson (1980) reported that the synchronization indexes of ANFs with CFs below 1 kHz were between 0.7 and 0.9. These indexes sound high but could cause jitter in the order of hundreds of microseconds at lower CFs. These temporal values are larger than those for human perception found by Mills.

In early physiological studies, the physiological responses of bushy cells in the AVCN, which receive impulses from ANFs, were thought to be similar to ANFs and behave like simple repeaters (e.g. Blackburn and Sachs 1989). However, Joris et al. (1994) revealed the higher tendency of cells to phase lock to low frequency tones such as enhanced synchronization and nearly perfect entrainment. Fig. 1 (Left) shows the synchronization for cells in the AVCN. The data are plotted on an expansive logarithmic scale that has an equal variance axis. The solid lines represent the range of indexes observed in ANFs by Johnson (1980). ANFs have indexes of less than 0.9 while 75 % of presumed bushy cells with CFs below 700 Hz have indexes that are greater than 0.9. Higher indexes over 0.9 can decrease jitter in impulses. Fig. 1 (Right) shows the entrainment for the cells discussed above. ANFs are represented as plots of crosses (+) and have entrainment indexes that are about 0.8 at lower CFs decreasing systematically with frequency, while many of the presumed bushy cells have nearly perfect entrainment indexes up to about 700 Hz. This means the bushy cells tend to fire with each stimulus cycle at lower CFs.

Bushy cells are connected by numerous synaptic terminals, which are of several types (Cant 1996). Especially striking terminals are a few large endbulbs of Held on spherical bushy cells (SBCs). Ryugo and Sento (1996) reported that each fiber gave rise to a single endbulb of Held. A single SBC has at most two endbulbs of Held on it, and the convergent endbulbs arise from fibers of the same SR (spontaneous discharge rate) group. As the physiological properties of a single SBC were thought to be similar to those of an ANF, its properties have also been considered to be dominated by a few endbulbs of Held despite the presence of many smaller terminals from ANFs (Cant 1996; Young 1998). However, globular bushy cells (GBCs) located more posteriorly in the AVCN receive a greater number of smaller somatic terminals, i.e. modified endbulbs, from ANFs (Cant 1996, Yin 2002).
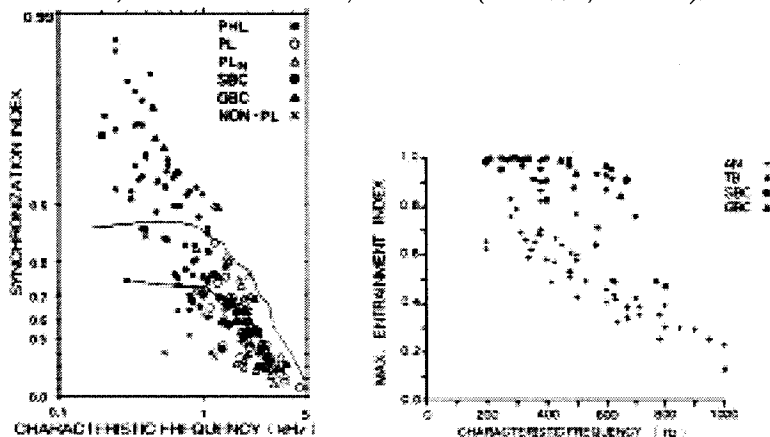

Fig. 1. *Left*: Synchronization index in ANFs and AVCN cells protted against CF. The ordinate designates (1-syn.) on a logarithmic scale. The area between solid lines indicates the range of indexes of ANFs from Johnson (1980). *Right*: Entrainment index in ANFs (crosses,+) and AVCN cells (the others). These data from Joris et al. (1994).

4 Simulations using computational model

If it is clear that bushy cell response differs from that of ANFs, a large endbulb does not function as a one-to-one relay even at low CFs where the endbulbs are largest. An important question is the mechanism by which bushy cells achieve enhanced phase locking. One way to obtain the enhanced phase locking is to have the cell behave as a coincidence detector with a number of presynaptic auditory nerve inputs with similar CFs (Yin 2002). Also, a postsynaptic bushy cell requires coincident input spikes before it generates an output spike (Joris et al. 1994). They showed that a simple "shot-noise" model (Colburn 1996) could mimic the enhanced phase locking of bushy cells to pure tones at CF. Rothman, Young, and Manis (1993) and Rothman and Young (1996) studied various combinations of inputs and strength to simulate the physiological responses of bushy cells using a computational model similar to a point-neuron model (Colburn 1996). These models suggested that utilizing subthreshold inputs and required coincidence to

3

evoke a spike is useful in enhancing synchronization. Although they demonstrated various cases, these were not sufficient for perfect entrainment.

This study demonstrates the mechanism by which a single neuron attains perfect entrainment as well as synchronization through using a computational model. In particular, we derive the quantitative relation between the number of input terminals (*n*) and the number of required input events (*k*) to evoke a spike by analyzing the relation between input and output entrainment indexes. The model cell used in this study was a type of shot-noise model. The model cell was connected by *n* input-terminals with the same CF. It generated an output spike with at least coincident *k* input-events. An input-event means a firing at a presynaptic fiber. The model cell potential in response to an input is described by the following equation.

$$V(t) = a \cdot e^{-t/\tau},$$ (3)

where *V(t)* denotes the postsynaptic potential (PSP) at time *t*. The PSP decays exponentially to the resting potential. τ denotes the time constant of PSP and *a* denotes the subthreshold amplitude of PSP. Output firing occurs when the total PSP potential exceeds a threshold level. This model cell operates as a kind of coincidence detector because input-events must occur close together to cause the cell to cross the threshold. The membrane potential is reset to zero following output firing and the model cell does not respond to any input during the refractory period. The model cell receives input spike trains that simulate the primary-like pattern of ANFs including their synchronization and entrainment properties.

5 Results

We conducted some simulations to investigate the mechanism that improves phase locking in a single cell with various combinations of parameters *n* and *k*. We will discuss simulation results where *k* = 2 which means that the model cell needed at least 2 simultaneous input-events to evoke an output spike. Other values of *k* yielded similar results to this case. The model cell had τ set to 0.5 (ms) and the refractory period to 1.5 (ms), which were the same values as those used by Joris et al. Fig. 2 has the results for synchronization (Left) and entrainment (Right) of the model cell (*k* = 2) with various parameters of *n*. The indexes of input spike trains that simulate the primary-like properties of ANFs at CFs are plotted as closed circles "●". The number of input terminals (*n*) is *n* = 2, 3, 5, and 10. The indexes of the model cell in response to each *n* are represented by the symbols "▽", "○", "□", "◇", respectively. Every plot, including input, represents the mean and standard deviation of each index obtained through a hundred trials of simulation.

In Fig. 2 (Left), the abscissa indicates CFs and the ordinate designates (1 − sync.) on a logarithmic scale. The simulations revealed that the synchronization indexes of all output were higher than those of input at CFs below 700 Hz, and the indexes become higher as parameter *n* became larger. The synchronization simulation was influenced by the fixed refractory period (1.5 ms) because the cell fired according to the refractory period at CFs above 700 Hz. Therefore, the results for CFs above 700 Hz were not significant. In Fig. 2 (Right), the abscissa designates CFs and the ordinate designates entrainment indexes. The simulation

4

revealed that the entrainment indexes for output with $n = 2$, "∇", were lower than those for input at all CFs, and the indexes for output with $n = 3$, "$\bigcirc$", were similar to those for input at low CFs below 600 Hz. When $n = 10$, "$\diamondsuit$", simulation revealed nearly perfect entrainment indexes at CFs below 600 Hz. Entrainment was also influenced by the fixed refractory period (1.5 ms) due to the same reasons as synchronization. The indexes declined rapidly at CFs above 600 Hz.
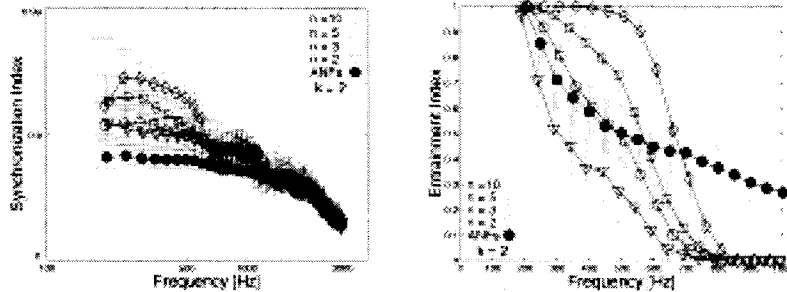

Fig. 2. Means and standard deviations of the synchronization and entrainment indexes in the model cell with $n = 2, 3, 5$, and 10 and $k = 2$. Closed circles denote the indexes for ANFs. *Left*: Synchronization indexes at CFs below 700 Hz are higher as the n becomes larger. *Right*: Entrainment indexes at CFs below 600 Hz are nearly perfect when $n = 10$.

6 Discussion

We investigated transitions in synchronization and entrainment of the model cell in these simulations by changing parameter n while fixing parameter k to other values ($k = 1, 2, 3, \cdots$). The synchronization results indicated that at low CFs below 700 Hz, the indexes increase monotonously from the index level of ANFs as parameter n increase, even when $n = 2$. These plots were good fits for the physiological data in this CF range. For other k parameters, simulations appeared to have a similar tendency. The mechanism for coincidence detection with larger n to improve synchronization is useful as Joris et al. (1994) predicted in their study. However, in enhancing temporal information it is important to satisfy both synchronization and entrainment. Entrainment results revealed that indexes do not increase monotonously like they do for synchronization. When parameter $k = 2$, only the entrainment indexes of $n = 10$, "$\diamondsuit$", were nearly perfect at CFs below 600 Hz and this was a good fit with the physiological data. It seems that a mechanism for coincidence detection with a much larger n is needed compared with k to obtain perfect entrainment. These results suggest the possibility of a firing mechanism with multiple inputs on a single neuron in the AVCN that enhances temporal information. This does not seem to be consistent with the general agreement obtained from anatomical studies. If results obtained through simulations are plausible, we have to consider the possibility that bunches of smaller synaptic terminals may also be involved in the mechanism that enhances temporal information on a single neuron in the AVCN.

5

Then we considered a way of mathematically estimating the value of n and that of k to enhance temporal information. To achieve this, we modified the equation for the entrainment index so we could add the information for the stimulus period. The modified entrainment index G is defined by the following equation.

$$G = h_F / N_f,\qquad(4)$$

where N_f denotes the number of times stimulus period (1/CF) occurred during the entire stimulation, instead of the total number of intervals of spikes (N_s). h_F is the same as in Eq. 2. Hence, G denotes the ratio for the number of times ISI occurred over the number of times the stimulus period (1/CF) occurred. Fig. 3 (Left) shows modified entrainment converted from the normal one in Fig. 2 (Right). Then, we can define the modified entrainment index G of the ith input terminal as the probability $0 \le P_{G_i} \le 1$, $i \in N$. Events of firing at input terminals are regarded as independent. An output event at a cell is considered to be generated by the joint event of firing at the input terminals. In the case of two input terminals ($n = 2$) and two input events ($k = 2$) simultaneously required to output a spike, output probability $P_{G_{out}}$ is given by the joint probability $P_{G_1} \cdot P_{G_2}$ of input probability P_{G_1} and P_{G_2} because coincidence of ISIs from both input terminals allows a cell to output an ISI. As simulations show, the entrainment of output is not satisfied when $n = 2$ and $k = 2$. We need to add other input terminals to increase $P_{G_{out}}$. Since a parameter n greater than k increases the number of occasions to generate ISIs of output with no ISI from inputs terminals, output probability $P_{G_{out}}$ is approximated to the worst case. The input probabilities are regarded as having the same probability P_{G_i} because terminals on a single cell probably belong to the same SR group (Ryugo and Sento 1996). Therefore, the quantitative relation between n and k is given by the following estimate.

$$P_{G_{out}} = \sum_{m-k}^{n}\binom{n}{m} \cdot P_{G_i}{}^m \cdot \left(1 - P_{G_i}\right)^{n-m}.\qquad(5)$$

This provides us with an approximation for the least number of input terminals (n) on a single cell when the number of required input events (k) to evoke a spike is given. Fig. 3 (Right) denotes output probability and shows good approximation to the modified entrainment G in Fig. 3 (Left) at CFs below 600 Hz. It suggests that a single cell with a CF of 400 Hz should have at least 10 input terminals to maintain the modified entrainment index so that is greater than 0.9. The output probability does not fit to the modified entrainment index at CFs above 600 Hz because this estimate does not take the refractory period into account.

7 Conclusion

This study demonstrated the mechanism through which a single neuron enhanced temporal information from the viewpoint of entrainment as well as synchronization using a computational model. As a result of simulation, a model with multiple-input configurations yielded enhanced synchronization and nearly perfect entrainment at low CFs. The relation between the number of input terminals and the number of

input events to output a spike was derived quantitatively to maintain enhanced temporal information against the primary-like behavior of inputs from ANFs. The results suggested the possibility of a firing mechanism that had multiple inputs on a single neuron in the AVCN.
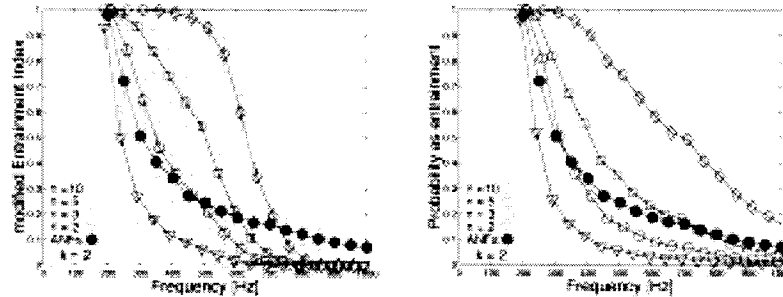

Fig. 3. *Left*: Modified entrainment indexes are converted from the normal entrainment indexes. *Right*: Output probability is calculated by Eq. 5 with $n = 2, 3, 5$, and 10 and $k = 2$. Input probability refers to the modified entrainment indexes of the ANFs.

References

Blackburn, C.C. and Sachs, M.B. (1989) Classification of unit types in the anteroventral cochlear nucleus: PST histograms and regularity analysis. J. Neurophysio., 62 (6), pp.1303-1329.

Cant, N.B. (1996) The cochlear nucleus: neuronal types and their synaptic organization. In: D.B. Webster, A.N. Popper and R.R. Fay (Eds.), *The Mammalian Auditory Pathway: Neuroanatomy*, Springer-verlag, New York. pp. 66-116.

Colburn, H.S. (1996) Binaural Models. In: H.L. Hawkins, T.A. McMullen, A.N. Popper and R.R. Fay (Eds.), *Auditory Computation*. Springer-verlag, New York. pp.332-400.

Johnson, D.H. (1980) The relationship between spike rate and synchrony in responses of auditory nerve fibers to single tones. J. Acoust. Soc. Am. 68, pp. 1115-1122.

Joris, P.X., Carney, L.H., Smith, P.H. and Yin, T.C.T. (1994) Enhancement of neural synchronization in the anteroventral cochlear nucleus. I. responses to tones at the characteristic frequency. J. Neurophysiol., 71(3), pp. 1022-1036.

Mills, A.W. (1958) On the minimum audible angle. J. Acoust. Soc. Am. 30, pp. 237-246.

Rothman, J.S., Young, E.D. and Manis, P.B. (1993) Convergence of auditory nerve fibers onto bushy cells in the ventral cochlear nucleus: implications of a computational model. J. NeuroPhysiol., 70(6), pp. 2562-2583.

Rothman, J.S. and Young,E.D.(1996) Enhancement of neural synchronization in computational models of ventral cochlear nucleus bushy cells. Aud. Neurosci., 2, pp.47-62.

Ryugo, D.K. and Sento, S. (1996) Auditory nerve terminals and cochlear nucleus neurons: endbulbs of Held and spherical bushy cells. In: W.A. Ainsworth, E.F. Evans and C.M. Hackney (Eds.) *Advances in Speech, Hearing, and Language Processing, vol.3*, JAI Press, Connecticut

Yin, T.C.T. (2002) Neural mechanisms of encoding binaural localization cues in the auditory brainstem. In: D. Oertel, R.R. Fay and A.N. Popper (Eds.), *Integrative Functions in the Mammalian Auditory Pathway*, Springer-verlag, New York, Chap.4, pp. 99-159.

Young, E.D. (1998) Cochlear nucleus. In: *Synaptic Organization of the Brain (4th Ed.)*. Oxford Press, London.